International Journal of Pharmaceutics 651 (2024) 123732

Contents lists available at ScienceDirect

International Journal of Pharmaceutics

journal homepage: www.elsevier.com/locate/ijpharm

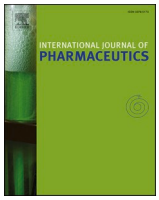

Semi-solid functionalized nanostructured lipid carriers loading thymol for skin disorders

Camila Folle [a,*], Elena Sánchez-López [a,b,*], Mireia Mallandrich [a,b], Natalia Díaz-Garrido [d,e,f], Joaquim Suñer-Carbó [a,b], Lyda Halbaut [a,b], Paulina Carvajal-Vidal [a], Ana M. Marqués [c], Marta Espina [a,b], Josefa Badia [d,e,f], Laura Baldoma [d,e,f], Maria Luisa García [a,b], Ana Cristina Calpena [a,b]

[a] Department of Pharmacy and Pharmaceutical Technology and Physical Chemistry, Faculty of Pharmacy and Food Sciences, University of Barcelona, 08028, Barcelona, Spain
[b] Institute of Nanoscience and Nanotechnology (IN2UB), University of Barcelona, 08028, Barcelona, Spain
[c] Department of Biology, Healthcare and Environment, Faculty of Pharmacy and Food Sciences, University of Barcelona, 08028, Barcelona, Spain
[d] Department of Biochemistry and Physiology, Biochemistry and Biomolecular Science, University of Barcelona, 08028, Barcelona, Spain
[e] Institute of Biomedicine of the University of Barcelona (IBUB), 08028, Barcelona, Spain
[f] Research Institute Sant Joan De Déu (IR-SJD), 08950, Barcelona, Spain

ARTICLE INFO

Keywords:
Lipid nanoparticles
Thymol
Nanostructured lipid carriers
Dermal
Acne

ABSTRACT

Acne constitutes one of the most prevalent skin disorder affecting both skin and mental health of patients. However, no cure has been developed so far. In this area, Thymol constitutes a potential candidate since it is able to restore the healthy microbiota of the skin. However, its permeation properties cause its fast elimination and, to avoid this problem, thymol has been loaded into nanostructured lipid carriers (TH-NLCs). Moreover, to increase the suitability of these systems for skin applications, several surface functionalization strategies of TH-NLCs had been assessed. Among the different molecules, phosphatidylcholine-TH-NLCs demonstrated to be safe as well as to provide high antioxidant activity in cellular studies. Therefore, to administer these systems to the skin, functionalized TH-NLCs were dispersed into a carbomer gel developing semi-solid formulations. Rheological properties, porosity and extensibility of TH dispersed in carbomer as well as phosphatidylcholine-TH-NLCs were assessed demonstrating suitable properties for dermal applications. Moreover, both formulations were applied in healthy volunteers demonstrating that gel-phosphatidylcholine-TH-NLCs were able to increase in skin hydration, decrease water loss and reduce skin sebum. Therefore, gel-phosphatidylcholine-TH-NLCs proved to be a suitable system for skin pathologies linked with high sebum generation, loss of hydration and high oxidation, such as acne vulgaris.

1. Introduction

Cutibacterium acnes (previously called *Propionibacterium acnes*) is known to play a dual role on healthy skin but also on pathogenic conditions (Byrd et al., 2018). An imbalance in the skin host-microbiome (especially *C. acnes*) has been demonstrated to lead to sebum level disorders. Therefore, the skin is more prone to be affected by endogenous or exogenous factors, leading to infection or inflammation, referred to dysbiosis (Ito and Amagai, 2022).

This is highly related with the physiopathology of acne, which is complex, being its main hallmarks the increase of sebum generation, duct hyperkeratinization, a rise of anaerobic bacteria, and inflammatory response (Bernales Salinas, 2021). Moreover, internal and external factors seem to be also involved in acne (Bharti and Vadlamudi, 2021). Acne vulgaris is defined as an oily skin pathology that affects 85 % of adolescents, often starts in preadolescence and persists into adulthood (Habeshian and Cohen, 2020). This disease is the eighth most prevalent pathology worldwide and it is tightly linked with a negative impact on mental health significantly affecting quality of life (Tayel et al., 2020), (Thiboutot and Del Rosso, 2013), (Bernales Salinas, 2021). The

* Corresponding authors at: Department of Pharmacy and Pharmaceutical Technology and Physical Chemistry, Faculty of Pharmacy and Food Sciences, University of Barcelona, 08028, Barcelona, Spain.
E-mail addresses: camilafolle@ub.edu (C. Folle), esanchezlopez@ub.edu (E. Sánchez-López).

https://doi.org/10.1016/j.ijpharm.2023.123732
Received 5 September 2023; Received in revised form 19 December 2023; Accepted 20 December 2023
Available online 22 December 2023

treatment recommendations depend on the severity of the condition but it would often require topical antibiotics and retinoids (Dréno et al., 2020). In addition to the problem of antibiotic resistance, treatments are concomitant with skin dryness and irritation in some patients which may reduce adherence and affect the treatment results in a negative manner. Moreover, antibiotics potentially damage the entire skin microbiome, therefore the skin remains unbalanced and without defense to external pathogens, being prone to other disorders. Therefore, treatments focused on patient comfortability constitute an unmet medical need.

In this area, natural compounds had demonstrated suitable patient acceptability. Furthermore, the use of natural compounds for skin application has been given broad attention lately, due to their ability to treat inflammation and infections, without negatively affecting the skin microbiome. Among them, Thymol (TH), is a natural monoterpene with a phenolic structure associated with several activities such as antioxidant, antimicrobial, antiseptic and anti-inflammatory (Nagoor Meeran et al., 2016; Najafloo et al., 2020; Pivetta et al., 2018). Studies developed by several authors (Briganti and Picardo, 2003) showed the capacity of TH to increase skin elasticity and porosity, which are essential on the healing processes. Despite its suitable pharmaceutical activity, TH is a monoterpene, which is also known to have permeation enhancer activity, since its molecule is able to disturb the lipids of the stratum corneum (SC) (Pham et al., 2016). For this reason, it may have difficultly to remain for long time inside the skin (Folle et al., 2021b, 2021a). Therefore, in order to increase TH activity for dermal application, lipid nanoparticles and specially nanostructured lipid carriers (NLCs), constitute a suitable solution able to encapsulate lipophilic compounds such as TH (Rincón et al., 2022). Moreover, NLCs, which constitute the second generation of lipid nanoparticles, are able to provide a prolonged drug release and may be functionalized using different molecules as well as incorporated into gelling systems.

In fact, NLCs are known be adhesive to the skin surface and to provide occlusive properties, related to their close contact with the stratum corneum (SC) superficial junctions while permeating, allowing superficial spreading of the encapsulated active (Khater et al., 2021). Moreover, due the lipid composition of NLCs, they have great affinity to the skin sebum, which may favour skin penetration in oily skin (Lauterbach and Müller-Goymann, 2015; Souto et al., 2020).

In previous studies developed by our group, we have demonstrated potential effects of thymol-loaded surface functionalized polymeric nanoparticles towards skin healing activity and microbiome friendly advantages (Folle et al., 2021a). In addition, TH loading into NLCs has also been demonstrated. Therefore, in this manuscript, functionalization of TH loaded NLCs using different strategies has been carried out based on the previously developed TH-NLC. Moreover, functionalized NLCs had been produced and characterized. The *in vitro* cell viability and antimicrobial efficacy has been demonstrated and they were dispersed into a carbomer gel. Functionalized-gel dispersed TH-NLCs were observed by transmission electron microscope and their biomechanical properties assessed in healthy volunteers.

2. Material and methods

2.1. Materials

Thymol (TH), Tween® 20 (TW), poloxamer 188 (PX), glycerin (GLY) and propylene glycol (PG) were purchased from Sigma Aldrich (Madrid, Spain). Glyceryl behenate (Compritol CG 888 ATO, C888) and PEG-8 Caprylic/Capric Glycerides (LAS MB, LAS) were gifted by Gattefossé (Cedex, France). Chitosan (CS) was supplied by HMC+ (GmbH, Saale, Germany), phosphatidylcholine (PL) was acquired from Lipoid® (GmbH, Ludwigshafen am Rhein, Germany) and Carbopol® 934, (C934, carbomer) was purchased from Fagron Iberica (Barcelona, Spain). Double-distilled water was used after filtration in a Millipore system (Molsheim, France). All other chemicals and reagents used in the study were of analytical grade.

Culture media Brain Heart Infusion (BHI), Clostridium reinforced medium (CRM), Tryptone Soy Agar (TSA) and Sabouraud Dextrose Agar (SDA) were purchased from Oxoid (Basingstoke, UK). DMEM (Dulbecco's Modified Eagle's Medium) was purchased from ThermoFisher, Bereńs (cosmetic diluent) was acquired from Scharlab (Barcelona, Spain), MTT (3-(4,5-Dimethylthiazol-2-yl)-2,5-diphenyl tetrazolium bromide) from Sigma-Aldrich (St. Louis, MO, USA), DMSO (99 % dimethyl sulfoxide) and DPPH (2,2-diphenyl-1-picrylhydrazyl) from Sigma-Aldrich (Barcelona, Spain).

2.2. Preparation of TH-NLCs

Thymol-loaded lipid nanoparticles (TH-NLCs) were produced by high energy procedure with the ultrasonication probe (US) by using a Sonics Ultrasonic®probe (Sonics & Materials Inc., CT, USA). Briefly, to produce TH-NLC with TW (TH-NLC-T-), the aqueous phase containing TW was heated above 80 °C as well as the lipid phase containing 0.5 % of TH and 2 % of total lipid mixture. The aqueous phase was then added into the lipid phase and a pre-emulsion was generated using an Ultra-Turrax T25 (IKA, Staufen, Germany) for 2 min by at 5000 rpm, followed by ultrasonication during 20 min at 40 % amplitude and immediately cooled down under cold running water for 5 min (Carvajal-Vidal et al., 2019; Rincón et al., 2018). Samples were kept overnight for further characterization analysis.

Surface modification of TH-NLCs was performed by replacing TW with 0.8 % of Poloxamer 188 (TH-NLC-P-) or Phosphatidylcholine (TH-NLC-L-) and, additionally, to obtain positively charged NLCs, CS at 0.05 % (TH-NLC-T-C+, TH-NLC-P-C + and TH-NLC-P-C+) was added to the aqueous phase. The prior stock solution of CS was prepared in 1 % acetic acid (Folle et al., 2021a).

2.3. Characterization of functionalized TH-NLCs

The physicochemical characterization of TH-NLCs (Z_{av} and PI) was assessed by photon correlation spectroscopy (PCS) using a ZetaSizer Nano ZS (Malvern Instruments, Malvern, UK). The zeta-potential (ZP) was estimated by electrophoretic mobility using the same instrument. For these measurements, samples were previously diluted with Milli-Q water (1:20).

The thermal interaction study was assayed by means of differential scanning calorimetry (DSC). Briefly, TH alone, the blank mixture of the selected lipids and the lipid mixture blended with thymol were analysed as previously described elsewhere, with minimal modifications (Carvajal-Vidal et al., 2019; Folle et al., 2021b). The equipment was set up at 10 °C/min, running from 5 to 100 °C and the thermograms were acquired using a DSC823e System (Mettler-Toledo, Barcelona, Spain). Data were evaluated from the peak areas with Mettler STARe V 9.01 DB software (Mettler-Toledo, Barcelona, Spain).

2.4. In vitro antimicrobial efficacy

A suspension test was assayed to identify the antimicrobial activity of TH and the variable surface compositions of TH-NLCs, based on the method previously described (Folle et al., 2021a). Briefly, *C. acnes* was cultured in BHI medium for 48 h at 37 °C under anaerobic conditions using parches AnaeroGen® and indicator (Oxoid, Basingstoke, UK). The inoculum was prepared in PBS adjusted to optical density (OD) of 0.720 at 550 nm, using a UV–visible spectrophotometer (Shimazu, Kyota, Japan). Then, 100 μL was added to each sample of TH or TH-NLCs (900 μL) with the final concentration of 250 μg/mL. After 30 min incubated at 37 °C in a shaker incubator Innova 4080 (New Brunswick Scientific, NJ, USA), samples were neutralized (1:10) in Beren's cosmetic diluent for 15 min. Microbial count was performed in CRM agar dishes after incubation for 48 h under anaerobic conditions at 37 °C, using drop count method. Bacterial viability was expressed as CFU/mL (Messager et al.,

2001).

2.5. In vitro antioxidant activity

The free radical scavenging capacity of TH (0.5 %), PX (0.8 %) and PL (0.8 %) were evaluated alone or mixed, using DPPH assay, based on other authors with some modifications (Aman et al., 2013). Samples were placed into an Eppendorf® (1000 µL) and 100 µL of a DPPH stock solution (0.1 mM), previously prepared in methanol (80 %), were added. Tubes were incubated in the dark for 45 min, while placed onto a mechanical shaker. Then, samples were transferred into quartz cuvettes and measured using a spectrophotometer UV–VIS (Shimazu, Kyota, Japan). The absorbance was measured at 517 nm and data were calculated using the equation (1):

$$Scavenging\% = \left(\frac{(Ac - As)}{Ac}\right)x100 \quad (1)$$

where *Ac* and *As* are the absorbances of the control (DPPH) and of the samples, respectively.

2.6. In vitro cell viability assay

The cytotoxicity of TH-NLCs was assessed determining the cell viability of human epidermal keratinocyte cell lines (HaCaT), at variable concentrations, as previously described elsewhere (Folle et al., 2021a). Briefly, HaCaT cells were cultured in high glucose DMEM, supplemented with 10 % foetal bovine serum (FBS), 2 mM l-glutamine, 100 units/mL penicillin G and 100 µg/mL streptomycin. Cells were adjusted at a density of 2×10^5 cells/well in automated cell counter (Invitrogen® Countess®, ThermoFisher Scientific, Karlsruhe, Germany) and seeded in 96-well plates with 100 µL. Diluted samples were added to the plates, followed by incubation for 24 h at 37 °C and 5 % CO_2. Thus, the medium was removed and MTT was added at 0.25 % in PBS, to determine the cell viability. After 2 h incubation, the medium was discarded and replaced with 100 µL of DMSO (Diaz-Garrido et al., 2019). Cell viability was measured at wavelength of 570 nm in a Modulus® Microplate Photometer (Turner BioSystems Inc., Sunnyvale, CA, USA). Results were expressed as percentage of cell survival relative to untreated cells.

2.7. Preparation of semi-solid formulations

After elucidating the antimicrobial activity and the cell viability of the developed TH-NLCs, the most suitable formulation was dispersed into a gel in order to be applied in healthy volunteers, compared to free-TH gel. Carbomer gels (GC) were formulated by previously dissolving 0.5 % of Carbopol® in water under constant magnetic stirring and then adding propylene glycol (5 %). Then, TH-NLC suspension of free-TH were dispersed under continuous stirring and emulsified using Unguator® (Microcaya, Bilbao, Spain). The mixtures were allowed to stand overnight, and the pH was adjusted to obtain pH value between 5.0 and 5.5 with NaOH 2 N.

2.8. Morphology study

Functionalized TH-NLCs as well as TH-NLC-L- dispersed in the gelling system were observed by transmission electron microscopy (TEM) on a JEM 1010 microscope (JEOL, Akishima, Japan). In order to perform this analysis, samples were stained using uranyl acetate at 2 % and placed on copper grids previously activated with UV light (Thiruchenthooran et al., 2022).

Additionally, images of the fresh gels (GC-TH and GC-TH-NLC-L-) were acquired with optical microscopy X63 (LEICA DFC300FX, Leica Microsystems, Wetzlar, Germany), to evaluate the gel matrix and homogeneity (Carvajal-Vidal et al., 2020a).

2.9. Stability of TH-NLCs formulations

Multiple light scattering was assessed in order to study the short-term stability of the developed functionalized TH-NLCs. The equipment employed was TurbiscanLab® Expert (Formulaction, Toulose. France). In order to perform the analysis, 20 mL of samples were placed into a glass vial and the backscattering profile was analyzed for 24 h (Esteruelas et al., 2022). For GC-TH-NLCs, measurements were also performed during storage for 1 month. Additionally, stability was studied up to 6 months, evaluating the organoleptic properties and pH measures of the gel formulations.

2.10. Microbial sterility of developed gels

The sterility of the gels (GC-TH and GC-TH-NLC-L-) was evaluated after formulation and prior to the *in vivo* study, using the methodology described elsewhere (Folle et al., 2021b). The testing protocol was developed following the European Pharmacopeia monographs specifications (2.6.12. Microbiological examination of non-sterile products: total viable aerobic count). Briefly, samples (0.1 g) were placed by inclusion onto TSA or SDA culture plates, incubated at 35 ± 2 °C for 3 days or at 28 ± 2 °C for 7 days, for bacteria and fungi/yeast, respectively.

2.11. Rheological studies

The rheology behavior of the developed gels (GC-TH and GC-TH-NLC-L-) was performed using a Haake Rheostress® 1 rheometer (ThermoFisher Scientific, Karlsruhe, Germany) connected to a thermostatic circulator Thermo® Haake Phoenix II + Haake C25P, computer system Haake RheoWin® Job Manager. The rotational analysis was performed with a plate-and-plate geometry (C60/2°Ti: 60 mm diameter, 2° angle). The shear stress (τ) was measured as a function of the shear rate (γ), and the viscosity ($\eta = f(\gamma)$) and flow ($\tau = f(\gamma)$) curves were recorded at 25 ± 0.1 °C. The system was set up to ramp-up period from 1 to 100 s^{-1} (3 min), constant shear rate (1 min) period at 100 s^{-1}, and ramp-down from 100 to 1 s^{-1} (3 min). The flow curve data were fitted to variable mathematical models to identify the best-fit profile provided experimentally from the rheological measurements. The viscosity (η, Pas) was determined from the constant shear at 100 s^{-1}. Results were processed using RheoWin® Data Manager software v. 4.91 (Suñer-Carbó et al., 2017).

2.12. Extensibility profile

To determine the extensibility (or spreadability) of the semisolid formulations, approximately 0.5 g of the sample were placed onto the gap holder and the cover-slide was placed on top. The study was performed at room temperature under compression, by increasing applied weights (5, 10, 20, 50, 100 and 150 g) on top of the cover-slide (26.06 g) for 60 s each, consecutively. The diameter of the circle obtained was measured (cm) for each weight applied. The increase in surface area (cm^2) was calculated as a function of the increasing weights applied (Carvajal-Vidal et al., 2020b). The experiment was run in triplicate and data was calculated by the equation (2):

$$E = \frac{\pi.(d)^2}{4} \quad (2)$$

where *d* is the average diameter measured in different directions.

2.13. Swelling capacity

To determine the swelling capacity of the developed gels (GC-TH and GC-TH-NLC-L-), approximately 1 g of the gels were weighed and dried in an oven at 40 °C until constant weight. Gel swelling was studied using phosphate buffers at pH 5.5, 7.4 and 8. These were transferred (0.5 mL)

into the sample tubes, incubated in a water bath (32 °C) for 3 min, and then centrifuged at 10000 rpm for 3 min. The supernatant water was dried, and the weight was recorded. This procedure was repeated cyclic until constant weight (Silva et al., 2023). The experiment was run in triplicate and data were used to calculate the swelling ratio (SR) by the equation (3):

$$SR = \frac{Ws - Wi}{Wi} \quad (3)$$

where, *Ws* presents the weight of the swollen gel and *Wi* the initial dried weight.

2.14. Porosity

The porosity of gels were studied by the solvent substitution method, following the same description of the swelling experiment, but using absolute ethanol instead of buffers. The loss of weight was recorded at each time. The porosity calculated by the equation (4):

$$P\% = \left(\frac{(W2 - W1)}{d.V}\right)x100 \quad (4)$$

where, *Wi* presents the weight of the fresh initial gel and *Ws* the weight of the sample each time, *d* is the density of absolute ethanol and *V* is the volume of the gel applied.

2.15. In vivo skin biomechanical properties of developed gels

The study of the biomechanical properties of the semisolid formulations was approved by the Ethics Committee of University of Barcelona (under the code IRB00003099). It was carried out by evaluating the *trans*-epidermal water loss (TEWL) measurement DermaLab® module (Cortex Technology) and skin hydration by Corneometer® (CM 825, C + K electronic, Courage-Khazaka electronic GmbH, Cologne, Germany). The measurement was determined prior and after the application of different formulations in a climate-controlled room (ambient temperature 25 ± 2 °C, relative humidity 45 %) at several timepoints. The volunteers (n = 12) were allowed a 30 min adaptation period prior to the measurements. Abnormalities in the structures related to disruption of the epidermal permeability barrier function were assayed by TEWL (g/cm^2·h). Statistical data were processed by GraphPad® using ANOVA non-parametric system, Wilcoxon paired test (Carvajal-Vidal et al., 2020b).

Another study was performed to evaluate the skin sebum levels of participants with oily acne-prone skin (n = 10) were assessed by Sebumeter® (Cutometer® dual MPA 580, C + K, Courage-Khazaka electronic GmbH, Cologne, Germany). Measurements were taken prior to application (basal levels) and along 1.5 h, on the forehead of the volunteers. Sebum quantification was given in μg/cm^2. Statistical data was processed by GraphPad® Prism 6, using ANOVA non-parametric system Wilcoxon paired test.

3. Results and discussion

3.1. Physicochemical characterization of functionalized TH-NLCs

The interaction studies of the lipid mixture, solid lipid and liquid lipid (7:3) and the encapsulated TH, were evaluated by DLS (Fig. 1A). Results showed that by adding TH, there is minimum displacement of the melting point of the mixture by 2 °C. In order optimize TH-NLC formulations, the surface were modified using different surface functionalization approaches. Several molecules were used in order to modify NLC surface (Tween® 20, TW; Phospholipid, PL; Poloxamer 188,

Table 1
Physical and chemical characterization of TH-NLCs surface-functionalized.

	Evaluated Parameters		
	Z_{av} (nm)	PI	ZP (mV)
TH-NLC-T-	270.1 ± 9.8	0.120 ± 0.001	−18.3 ± 0.9
TH-NLC-L-	260.9 ± 5.2	0.196 ± 0.005	−37.5 ± 1.2
TH-NLC-P-	280.2 ± 1.2	0.219 ± 0.014	−14.4 ± 1.4
TH-NLC-T-C+	352.0 ± 4.4	0.262 ± 0.035	+30.3 ± 1.1
TH-NLC-L-C+	330.1 ± 4.1	0.292 ± 0.032	+42.3 ± 2.6
TH-NLC-P-C+	312.8 ± 1.9	0.293 ± 0.021	+13.7 ± 1.3

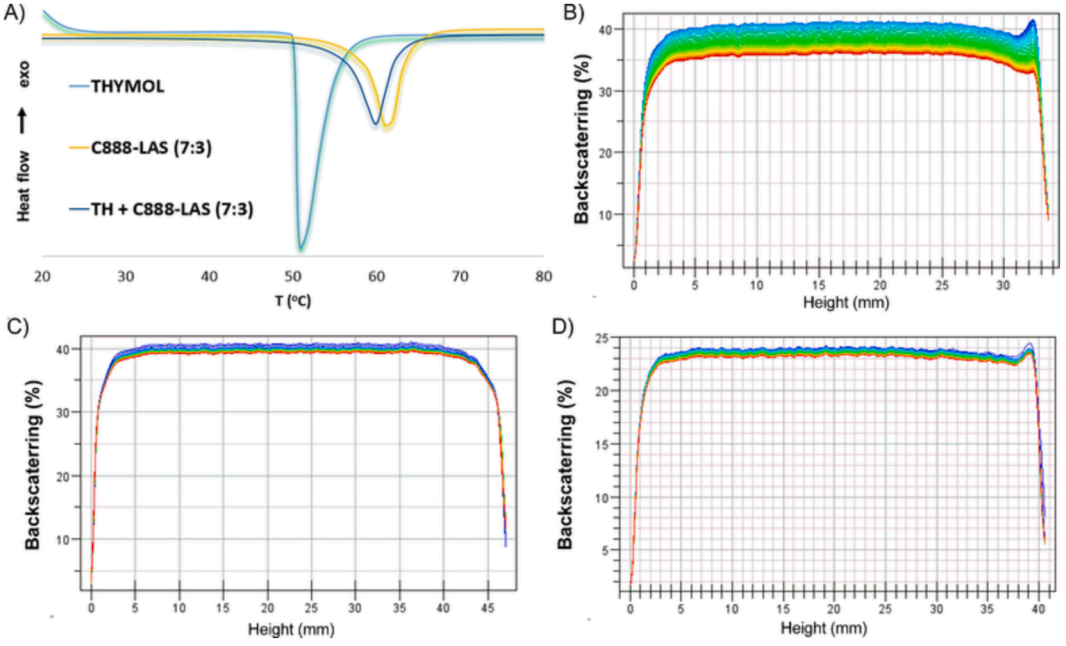

Fig. 1. Differential scanning calorimetry of TH and lipid mixture and stability of TH-NLCs. (A) Differential scanning calorimetry (B-D), Stability of surface functionalized TH-NLCs, analyzed by the backscattering signal measured by Turbiscan® Lab for (B) TH-NLC-L- (C) TH-NLC-T-C+ (D) and TH-NLC-L-C + Scans were performed from the bottom to the top of the vial, measured every hour for 24 h, represented from blue to red lines. (For interpretation of the references to color in this figure legend, the reader is referred to the web version of this article.)

PX; Chitosan, CS). The results of the obtained TH-NLCs are displayed in Table 1 where it can be observed that the use of either PL or positively charged compounds (CS) have increased the ZP value. Moreover, it can be observed that CS functionalization increases the average particle size of TH-NLCs, since CS is attached to the surface, surrounding the NLCs. CS is a positively charged polysaccharide which forms a polymeric layer surrounding the lipid particle via electrostatic binding. Previous authors stated that the biding cloud be via hydrogen bonding between the polysaccharide and of NLC glyceride head groups (Luo et al., 2011).

3.2. Stability of TH-NLCs formulations

The short-term stability was predicted by analyzing the backscattering profile of TH-NLCs formulations, measured by Turbiscan®Lab (Fig. 1**B-D and** S1.Fig. 1**A-C**). The behavior of TH-NLC-L- (Fig. 1**B**) was very similar to the one of TH-NLC-T- (S1.Fig. 1**A**) which, along storage, might lead to flocculation (with differences below 10 %). However, when these particles are coated with CS (Fig. 1**C and D**), this phenomenon was reduced, which may maintain the particles more stable, along storage, avoiding aggregation. In both cases, the ZP values were higher for the positively charged than the negatively charged. Previous authors also stated that NLC surface covered CS improved stability of the nanosystem (Choi et al., 2016). In the other hand, the formulations TH-NLC-P- and TH-NLC-P-C+ (S1.Fig. 1**B and C**, respectively), the particles show an initial sedimentation phenomenon (below 10 %), presenting minimal differences between them. In fact, for these last two formulations the ZP was lower either for negatively or positively charged, therefore, being less stable than the previous ones.

3.3. In vitro antimicrobial efficacy of TH-NLCs

The antimicrobial activity of different surface composition of TH-NLCs were evaluated by suspension test, for 30 min incubation with *C. acnes*. Results showed that TW on the surface provides stronger activity than PL or P (Fig. 2**A**), with could be related to its strong detergent properties. In the case of the positively charged, on the one hand, the ones containing CS (TH-NLC-T-C + and TH-NLC-L-C+), obtained similar results comparing to the negatively charged ones. When the surface modified TH-NLCs were exposed to *C. acnes* for 30 min, there were minimal differences between the activity of all formulations tested, not statistically significant.

3.4. In vitro cell viability of TH-NLCs (HaCaT)

The cell viability was studied in HaCaT-cell line using TH-NLCs at several concentrations (2, 10 and 20 μg/mL), performed by MTT. Fig. 2**B** shows that TH-NLC-T- presented a slight cytotoxicity when compared to the other formulations. However, the same composition but further

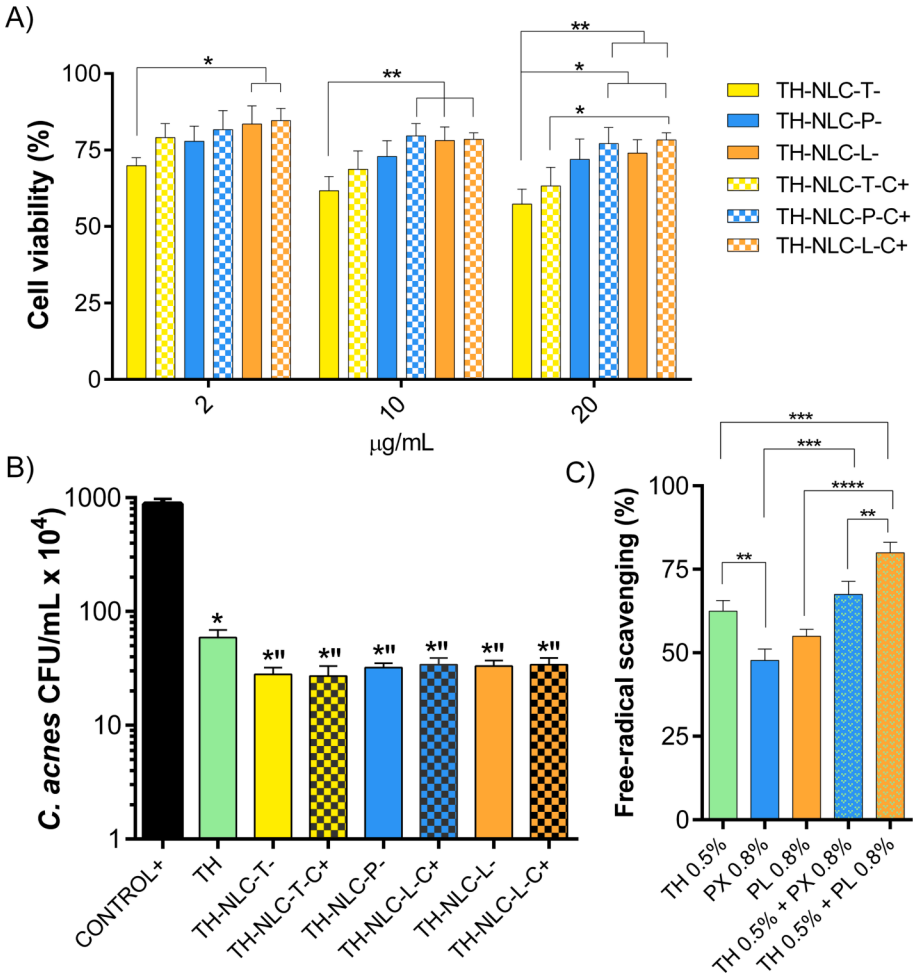

Fig. 2. Efficacy studies of the developed surface functionalized TH-NLCs. (A) Cell viability assay performed by MTT assay in HaCaT-cell lines at variable concentrations of TH-NLCs. Data are expressed as mean ± SD. Statistical analysis one-way ANOVA, Tukeýs multiple comparison test analyzed for each concentration tested (*p < 0.05, and **p < 0.01). (B) Antimicrobial activity by suspension test using *C. acnes* (30 min treatment). Statistical analysis *t* test against (*) control and (“) TH, p < 0.0001. (C) Antioxidant activity of free compound performed by DPPH for the concentrations used in the formulations. Statistical analysis one-way ANOVA, Tukeýs multiple comparison test (**p < 0.01, ***p < 0.001 and ****p < 0.0001).

covered by CS, showed a cell viability increase, statistically significant. When the surface of TH-NLCs were modified, by replacing TW with either PX or PL, the cell viability was improved significantly, and even more when both were also covered by CS. In fact, the highest cell viability can be observed at 2 μg/mL, with higher significance for the particles with PL and/or CS on the surface. Therefore, TW can be considered slightly cytotoxic to this cell line, when used at high concentrations, and for this reason, variable compositions of NLCs were studied in this work, to find the most suitable formulation for dermal application. Previous authors stated that the lipid NPs cytotoxicity in HaCaT-cell line are strongly related to the type and concentration of the surfactant used (Chauhan et al., 2020; Maupas et al., 2011). However, depending on the concentration of total lipids applied to the cells, could possibly be associated to lipid peroxidation (Szwed et al., 2020).

Therefore, the best stabilizer that presents lowest cytotoxicity was PL (TH-NLC-L- and TH-NLC-L-C +) and the addition of CS to each nanosystem also demonstrated to increase the cell viability of the tested formulations (TH-NLC-T-C+, TH-NLC-P-C + and TH-NLC-L-C +).

3.5. In vitro antioxidant activity

The antioxidant activity was evaluated for TH, PX and PL, alone and mixed, using the same concentrations determined for the formulation of the corresponding TH-NLCs, by measuring the free-radical scavenging capacity using DPPH. Results show that blending TH with both selected surface stabilizing agents, the antioxidant activity increased significantly (Fig. 2**C**). Moreover, PL was the best candidate for having the highest activity.

3.6. Gel dispersed formulations

The surface functionalized NLC chosen to be dispersed into the carbomer gel for further analysis was the NLC covered with PL (TH-NLC-L-) due to its lower cytotoxicity, higher surface charge, and higher antioxidant efficacy. Moreover, the fact that phospholipids are skin identical molecules, makes them suitable for skin barrier healing and reinforcement (Ramón et al., 2005). Moreover, the wound healing efficacy of nanoparticles of thymol functionalized with phosphatidylcholine was previously reported on an earlier work (Folle et al., 2021a).

The analysis performed by TEM confirms that functionalized NLCs possess a spherical shape and a smooth surface (Fig. 3**A-C**), which is in accordance with other publications observing NLCs (Thiruchenthooran et al., 2022). Moreover, TEM images confirm that the dispersion into a carbomer gel did not disrupt the NLCs structure and nanoparticles can be observed (Fig. 5**D**). Moreover, gel structure was also confirmed by optical microscopy (Fig. 3**E,F**).

3.7. Stability studies of developed gel formulations

When TH-NLCs were incorporated into a gel formulation (GC-TH-NLC-L-) (Fig. 4**A**), they presented an additional stabilization of the initial aqueous formulation (TH-NLC-L-) (Fig. 1**B**), where the backscattering signal has been improved, absent of creaming or flocculation. The measurements of the backscattering were also performed weekly for 1 month (Fig. 4**B**), presenting no relevant changes, where the NLCs were maintained stable being dispersed into the semi-solid formulation. Furthermore, the pH of the gel formulations (GC-TH and GC-TH-NLC-L-) were measured for 6 months at RT, remaining stable and with no color, odor, or appearance modification. The microbial sterility tested confirmed that no viable count of microorganisms in the incubated culture plate was found, which also confirms an antimicrobial activity of TH performing as preservative.

3.8. Rheological behaviour

The results of the rheological measurements showed that GC-TH and GC-TH-NLC-L- were dependent on shear rate (Fig. 5**A**). All formulations exhibited non-Newtonian behavior with a consistent decrease in viscosity by the shear rate increasing from 1 to 100 s^{-1}. The mathematical model Cross best-fitted with the resulting rheological profile, which provides a general model for shear-thinning materials, also defined as pseudoplastic. The apparent viscosity values, determined at the shear rate 100 s^{-1}, were found to be 1.7 ± 0.0 and 1.0 ± 0.0 (Pa.s), for GC-TH and GC-TH-NLC-L-, respectively (Table 2). The gel containing TH-NLCs incorporated has gained less viscosity due to the slightly acidic pH obtained when forming the NLCs, since GC viscosity is pH dependent.

3.9. Extensibility profile

The extensibility profiles of the developed gels (GC-TH and GC-TH-NLC-L-) were plotted as a function of the increased applied weight and were adjusted to the Hyperbola equation (Fig. 5**B**). The parameters of this profile, shown in Table 3, reveal the maximum value of extensibility (*Vm*) being 24.35 cm^2 and 22.80 cm^2, respectively, and the extensibility constant (*Km*) found to be 39.42 g and 58.41 g, respectively, which represents the weight needed to achieve half of the maximum extensibility. Results show that both gels present a wide spreadable surface with minimum weight applied, resulting in similar

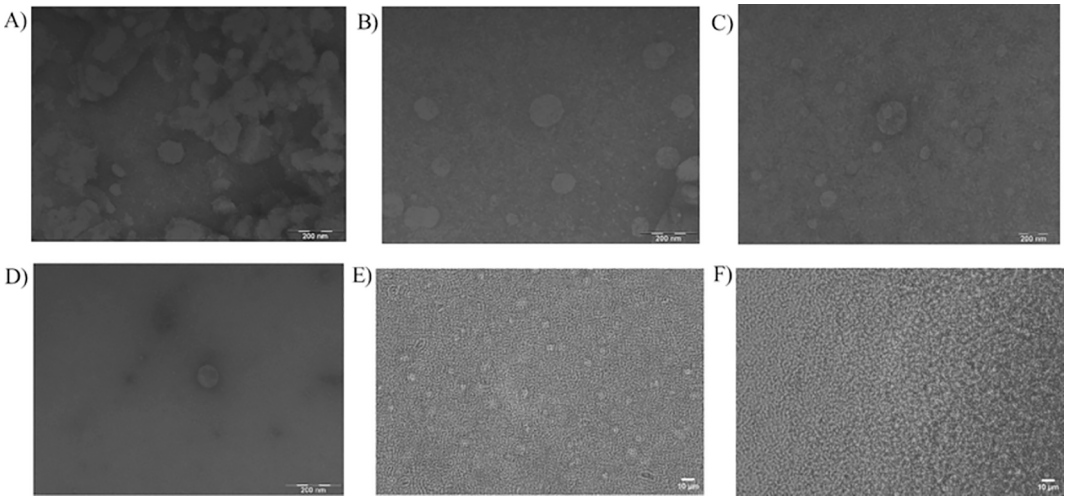

Fig. 3. Transmission electron microscopy of the developed nanostructured systems (scale bar 200 nm): A) TH-NLC-L-, B) TH-NLC-P-, C) TH-NLC-P-C + and the gel D) GC-TH-NLC-L-. Optical microscopy of the developed gels (scale bar 10 μM): E) GC-TH-NLC-L- and F) GC-TH.

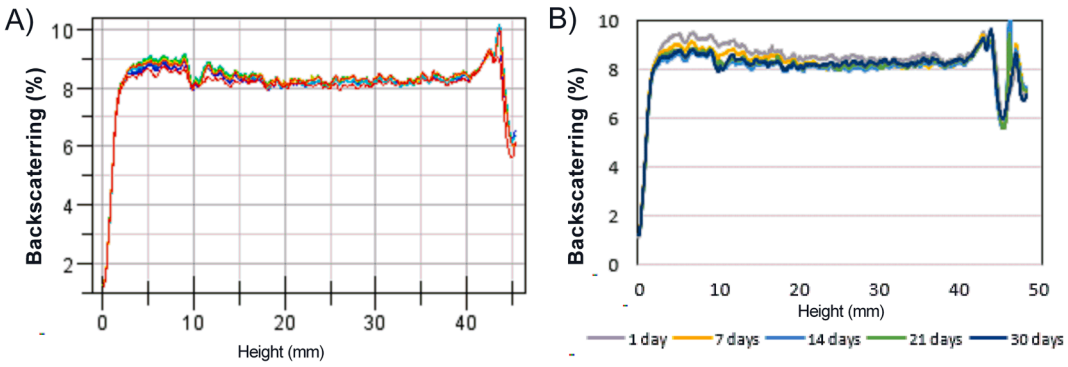

Fig. 4. Short-term stability of GC-TH-NLC-L-measuring the backscattering signal by TurbiscanLab®. (A) Scans performed for 24 h (1 scan/h) expressed from blue to red lines. (B) Weekly measurements for 1 month. (For interpretation of the references to color in this figure legend, the reader is referred to the web version of this article.)

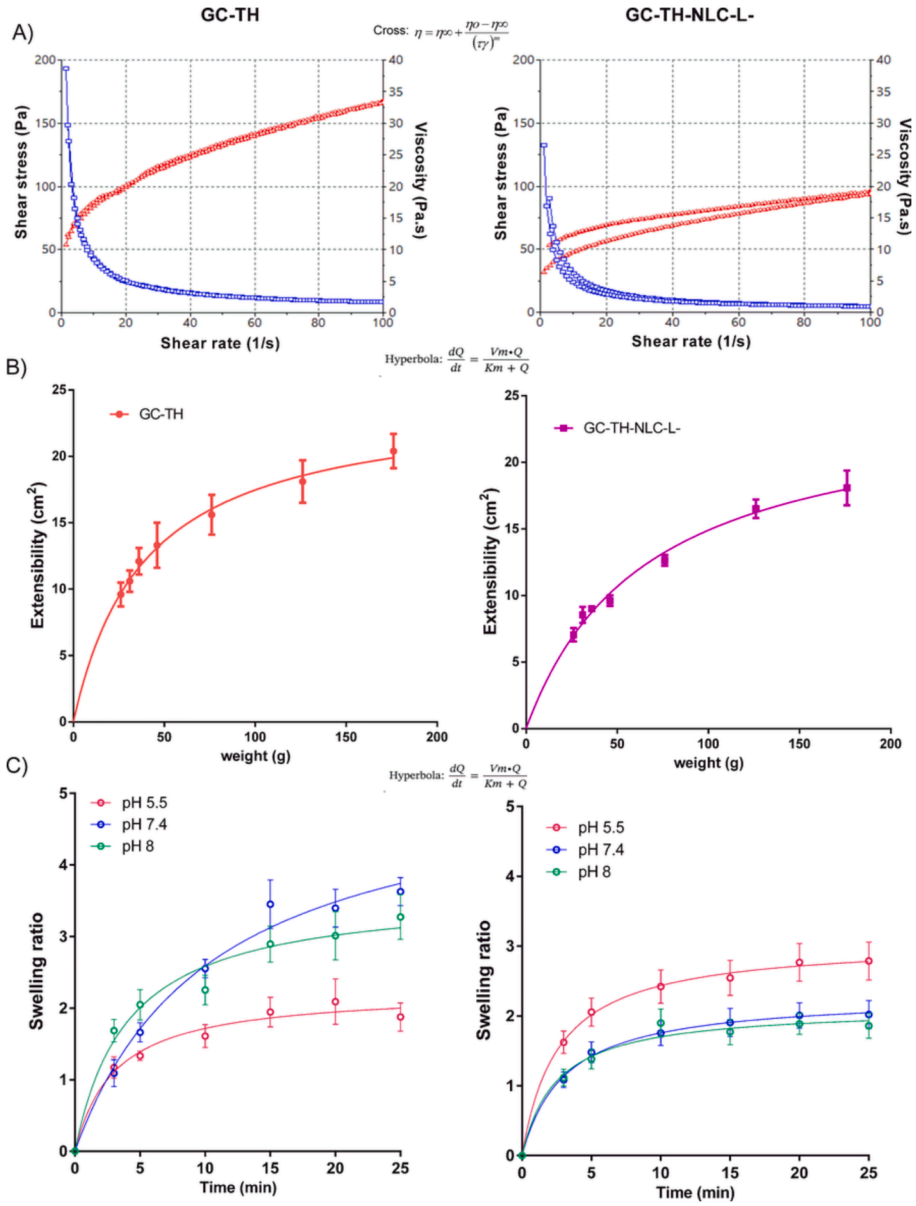

Fig. 5. Characterization of the developed gels, GC-TH and GC-HT-NLC-L-, displayed on the left and right, respectively. (A) Rheograms of gels with data adjusted to the best-fit mathematical model, Cross equation (η: apparent viscosity; $\tau 0$: shear stress; *Y:* deformation velocity; *K* consistency coefficient; *N:* flow behavior index). (B) Extensibility profile of the gels measured by increasing applied weights, adjusted to Hyperbola equation (*Vm*: maximum value obtained; *Km*: time taken to reach half of the maximum value). (C) The swelling (ratio %) capacity of the studied gels at variable pH conditions (5.5, 7.4 and 8), also adjusted to Hyperbola.

Table 2
Rheological behaviour and model applied for GC-TH and GC-TH-NLC-L-.

Sample	Viscosity (Pa.s)	Flow	Stretch model (Ramp up/down)	r (Ramp_up/down)
GC-TH	1.7 ± 0.0	Shear thinning	Cross/Cross	0.9990/0.9999
GC-TH-NLC-L-	1.0 ± 0.0	Shear thinning	Cross/Cross	0.9998/0.9999

Table 3
Extensibility parameters for GC-TH and GC-TH-NLC-L-.

	GC-TH	GC-TH-NLC-L-
Vm	24.35 ± 2.13	22.80 ± 2.01
Km	39.42 ± 3.38	58.41 ± 4.39
r^2	0.9321	0.9610

Vm: maximum extensibility value predicted by the hyperbola model;
Km: weight necessary to reach half of the maximum value.

values for *Vm*. However, the *Km* was 1.5 higher for GC-TH-NLC-L-, due to the presence of the lipid nanostructures. The extensibility of a gel improves the application to the damaged skin (Silva et al., 2023). Therefore, both formulations are suitable for the designed application.

3.10. Swelling capacity

The swelling capacity of the gels was determined at variable pH conditions, such as acidic (5.5) to mimic normal skin pH conditions, and also neutral (7.4) and alkaline (8.0) pH levels. Data of the average swelling ratio along time were plotted with the Hyperbola equation (Fig. 5**C**) and the parameters obtained are shown in Table 4. Results show that for GC-TH, the maximum swelling ratio capacity (*Vm*) can be observed at pH 7.4, increasing 5.32X of its initial dried weight, with a swelling constant (*Km*) of 10.55 min. on the other hand, for GC-TH-NLC-L-, the maximum swelling ratio was reached at pH 5.5, increasing 3.07X of the dried gel, and the constant was found to be 2.6 min. The obtained results have shown that the swelling behavior of the gels studied are different from each other, since the one containing TH-NLCs has lipids present (cream gel structure), while the other is a pure hydrogel. Additionally, we can observe that the variable pH conditions applied would also influence the swelling capacity of each gel.

3.11. Porosity

The porosity of the developed gels was determined by the solvent uptake of the dried gel with ethanol (Silva et al., 2023), resulting in 37.2 ± 3.9 and 83.6 ± 8.9 % for GC-TH and GC-TH-NLC-L-, respectively. Polymeric gels, such as carbomers, are networks of cross-linked chain structures where the pores are found in between. In the case of the gel containing the TH-NLCs incorporated into its matrix, the porosity was found to be more than twice higher (for GC-TH-NLC-L-) than for the simple gel network containing free TH. Therefore, the use of lipid nanocarriers in polymeric gel formulations would favor a prolonged release of TH when applied to the skin (Siboro et al., 2021; Thang et al., 2023).

Table 4
Swelling ratio parameters obtained by plotting data to Hyperbola equation.

	GC-TH			GC-TH-NLC-L-		
	pH 5.5	pH 7.4	pH 8	pH 5.5	pH 7.4	pH 8
Vm	2.25 ± 0.15	5.32 ± 0.33	3.63 ± 0.23	3.07 ± 0.31	2.3 ± 0.21	2.12 ± 0.12
Km	3.08 ± 0.25	10.55 ± 0.52	4.04 ± 0.25	2.62 ± 0.24	3.07 ± 0.28	2.48 ± 0.27
r^2	0.9325	0.9714	0.9458	0.9618	0.9617	0.9472

Vm: maximum swelling ratio predicted by the hyperbola model; *Km*: time taken to reach half of the maximum value.

3.12. In vivo skin biomechanical properties gel formulations

The skin *trans*-epidermal water loss (TEWL®) (Fig. 6 **A, D**) and the hydration of the SC (Corneometer®) (Fig. 6 **B, E**) were evaluated on volunteers' forearm, measuring the basal levels and for 2 h after application of the products. In the case of GC-TH (Fig. 6 **A, B**), results provided no statistically significant differences compared to the basal measure, not altering the skin barrier properties nor providing hydration effect, respectively. In contrast, GC-TH-NLC-L- (Fig. 6 **C, D**), provided a significantly decrease in TEWL values after 1 h and a slightly increased the SC skin hydration after 2 h, respectively, statistically significant compared to the basal measure. This result could be related to the film-forming properties of lipid nanoparticles which provided an occlusive effect, diminishing the internal water loss (Khater et al., 2021), also due to their high affinity with the intercellular lipids of the skin barrier. Previous authors also stated that NLC formulations present a film-forming behaviour in the skin due to their affinity to the SC lipids reordering it and that their incorporation into carbomer revealed promoting results in decreasing the TEWL values (Amasya et al., 2020).

The skin sebum was measured using Sebumeter® in the forehead, before and after application of the products (GC-TH and GC-TH-NLC-L-) during 1.5 h (Fig. 6 **C**, **F**, respectively). Results showed that both products successfully achieve sebum reduction activity, with statistically significant differences compared to the basal levels. In this case, GC-TH performed stronger activity and that could be expected due to the fast activity of free TH to reduce the sebum content, while TH-NLCs would need a longer timeframe to achieve the same efficacy. Therefore, results showed that both TH dosage forms have good sebum-regulator activity. However, a long-term treatment would be required to evaluate the efficacy of both products.

4. Conclusion

In the present study, TH was loaded into NLCs and their surface was functionalized using different molecules. The formulations were physicochemically characterized and cellular studies were undertaken demonstrating that TH loaded NLCs functionalized with phosphatidylcholine did not cause cytotoxicity and were able to provide high antioxidant activity. In addition, functionalized NLCs were dispersed into a gelling system (based on carbomer) developing a semi-solid formulation. The rheology and the gel extensibility studies demonstrated its potential for dermal applications. In addition, studies developed in healthy volunteers revealed that gel dispersed functionalized NLCs provide an increase in skin hydration and decreased water loss. Moreover, gel dispersed functionalized NLCs demonstrated to reduce skin sebum in healthy volunteers, thus constituting a promising treatment of skin sebum disorders, including acne vulgaris. In addition, its antioxidant activity is also beneficial for skin barrier healing conditions and the use of natural lipids and a natural antimicrobial active enables the treatment of the skin without completely damaging the host microbiome.

CRediT authorship contribution statement

Camila Folle: Formal analysis, Investigation, Methodology, Writing – original draft. **Elena Sánchez-López:** Conceptualization, Investigation, Writing – original draft. **Mireia Mallandrich:** Methodology, Supervision, Writing – review & editing. **Natalia Díaz-Garrido:** Investigation, Methodology. **Joaquim Suñer-Carbó:** Investigation, Methodology, Writing – original draft. **Lyda Halbaut:** Investigation, Methodology. **Paulina Carvajal-Vidal:** Investigation, Methodology. **Ana M. Marqués:** Funding acquisition, Investigation, Supervision, Writing – review & editing. **Marta Espina:** Investigation, Methodology.

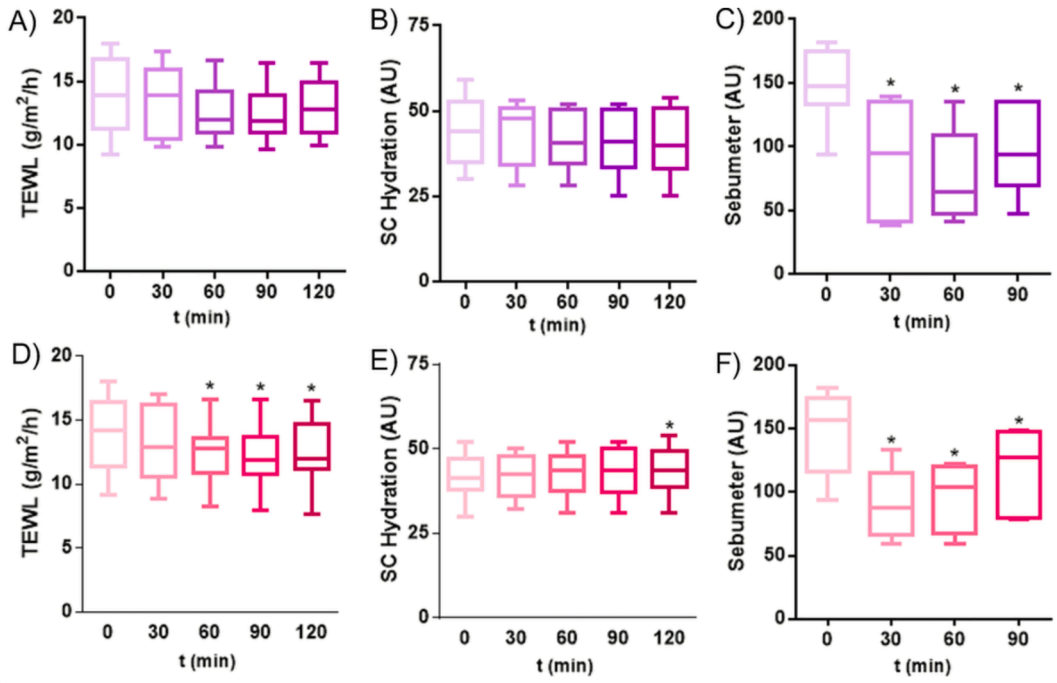

Fig. 6. Biomechanical properties of GC-TH (A-C) and GC-TH-NLC-L- (D-F) measured on the forearm of volunteers (n = 12) for the skin barrier function (TEWL®, A and D) and for hydration of SC (Corneometer®,B and D). Skin sebum measured on the forehead (n = 10) of oily skin volunteers (Sebumeter®, C and E). Statistical analysis performed as mean ± SD values, non-parametric Wilcoxon paired test comparing each measure against basal value (t0).

Josefa Badia: Funding acquisition, Investigation, Supervision. **Laura Baldoma:** Investigation, Methodology, Supervision. **Maria Luisa García:** Investigation, Methodology. **Ana Cristina Calpena:** Funding acquisition, Investigation, Supervision, Writing – review & editing.

Declaration of competing interest

The authors declare that they have no known competing financial interests or personal relationships that could have appeared to influence the work reported in this paper.

Data availability

No data was used for the research described in the article.

Acknowledgments

The authors would like to acknowledge Dr. Antonio Boix-Montañes for his assistance on the in vivo study. The authors wish to acknowledge the support of the Spanish Ministry under the project PID2021-122187NB-C32 and the support of the Generalitat of Catalonia (2017SGR1447). ESL wants to acknowledge the requalification system grants.

Appendix A. Supplementary material

Supplementary data to this article can be found online at https://doi.org/10.1016/j.ijpharm.2023.123732.

References

Amasya, G., Inal, O., Sengel-Turk, C.T., 2020. SLN enriched hydrogels for dermal application: Full factorial design study to estimate the relationship between composition and mechanical properties. Chem. Phys. Lipids 228. https://doi.org/10.1016/j.chemphyslip.2020.104889.

Aman, S., Moin, Shagufta, Owanis, M., Siddiqui, M.U., 2013. Antioxidant activity of thymol: Protective role in AAPH-induced hemolysis in diabetic erythrocytes. IJPSI. 2, 55–60.

Bernales Salinas, A., 2021. Acne vulgaris: role of the immune system. Int. J. Dermatol. 60, 1076–1081. https://doi.org/10.1111/ijd.15415.

Bharti, S., Vadlamudi, H.C., 2021. A strategic review on the involvement of receptors, transcription factors and hormones in acne pathogenesis. J. Recept. Signal Transduct. 41, 105–116. https://doi.org/10.1080/10799893.2020.1805626.

Briganti, S., Picardo, M., 2003. Antioxidant activity, lipid peroxidation and skin diseases. What's new. J. Eur. Acad. Dermatology Venereol. 17, 663–669. https://doi.org/10.1046/j.1468-3083.2003.00751.x.

Byrd, A.L., Belkaid, Y., Segre, J.A., 2018. The human skin microbiome. Nat. Rev. Microbiol. 16, 143–155. https://doi.org/10.1038/nrmicro.2017.157.

Carvajal-Vidal, P., Fábrega, M.J., Espina, M., Calpena, A.C., García, M.L., 2019. Development of Halobetasol-loaded nanostructured lipid carrier for dermal administration: Optimization, physicochemical and biopharmaceutical behavior, and therapeutic efficacy. Nanomedicine Nanotechnology. Biol. Med. 20, 1–10. https://doi.org/10.1016/j.nano.2019.102026.

Carvajal-Vidal, P., González-Pizarro, R., Araya, C., Espina, M., Halbaut, L., Gómez de Aranda, I., García, M.L., Calpena, A.C., 2020a. Nanostructured lipid carriers loaded with Halobetasol propionate for topical treatment of inflammation: Development, characterization, biopharmaceutical behavior and therapeutic efficacy of gel dosage forms. Int. J. Pharm. https://doi.org/10.1016/j.ijpharm.2020.119480.

Carvajal-Vidal, P., González-Pizarro, R., Araya, C., Espina, M., Halbaut, L., Gómez de Aranda, I., García, M.L., Calpena, A.C., 2020b. Nanostructured lipid carriers loaded with Halobetasol propionate for topical treatment of inflammation: Development, characterization, biopharmaceutical behavior and therapeutic efficacy of gel dosage forms. Int. J. Pharm. 585 https://doi.org/10.1016/j.ijpharm.2020.119480.

Chauhan, I., Yasir, M., Verma, M., Singh, A.P., 2020. Nanostructured lipid carriers: A groundbreaking approach for transdermal drug delivery. Adv. Pharm. Bull. 10, 150–165. https://doi.org/10.34172/apb.2020.021.

Choi, K.O., Choe, J., Suh, S., Ko, S., 2016. Positively charged nanostructured lipid carriers and their effect on the dissolution of poorly soluble drugs. Molecules 21. https://doi.org/10.3390/molecules21050672.

Diaz-Garrido, N., Fábrega, M.J., Vera, R., Giménez, R., Badia, J., Baldomà, L., 2019. Membrane vesicles from the probiotic Nissle 1917 and gut resident Escherichia coli strains distinctly modulate human dendritic cells and subsequent T cell responses. J. Funct. Foods 61. https://doi.org/10.1016/j.jff.2019.103495.

Dréno, B., Araviiskaia, E., Kerob, D., Andriessen, A., Anfilova, M., Arenbergerova, M., Forero Barrios, O.L., Bukvić Mokos, Z., Haedersdal, M., Hofmann, M.A., Khamaysi, Z., Kosmadaki, M., Lesiak, A., Roó, E., Zbranca-Toporas, A., Wiseman, M. C., Zimmo, S., Guerin, L., Fabbrocini, G., 2020. Nonprescription acne vulgaris treatments: Their role in our treatment armamentarium—An international panel discussion. J. Cosmet. Dermatol. 19, 2201–2211. https://doi.org/10.1111/jocd.13497.

Esteruelas, G., Souto, E.B., Espina, M., García, M.L., Świtalska, M., Wietrzyk, J., Gliszczyńska, A., Sánchez-López, E., 2022. Diclofenac loaded biodegradable nanoparticles as antitumoral and antiangiogenic therapy. Pharmaceutics 15, 102. https://doi.org/10.3390/pharmaceutics15010102.

Folle, C., Díaz-Garrido, N., Sánchez-López, E., Marqués, A.M., Badia, J., Baldomà, L., Espina, M., Calpena, A.C., García, M.L., 2021a. Surface-modified multifunctional

thymol-loaded biodegradable nanoparticles for topical acne treatment. Pharmaceutics 13, 1–23. https://doi.org/10.3390/pharmaceutics13091501.
Folle, C., Marqués, A.M., Díaz-Garrido, N., Espina, M., Sánchez-López, E., Badia, J., Baldoma, L., Calpena, A.C., García, M.L., 2021b. Thymol-loaded PLGA nanoparticles: an efficient approach for acne treatment. J. Nanobiotechnol. 19, 1–21. https://doi.org/10.1186/s12951-021-01092-z.
Habeshian, K.A., Cohen, B.A., 2020. Current issues in the treatment of acne vulgaris. Pediatrics 145, 225–230. https://doi.org/10.1542/PEDS.2019-2056L.
Ito, Y., Amagai, M., 2022. Controlling skin microbiome as a new bacteriotherapy for inflammatory skin diseases. Inflamm. Regen. 42 https://doi.org/10.1186/s41232-022-00212-y.
Khater, D., Nsairat, H., Odeh, F., Saleh, M., Jaber, A., Alshaer, W., Bawab, A. Al, Mubarak, M.S., 2021. and Transdermal Lipid Nanoparticles : A Review 1–43.
Lauterbach, A., Müller-Goymann, C.C., 2015. Applications and limitations of lipid nanoparticles in dermal and transdermal drug delivery via the follicular route. Eur. J. Pharm. Biopharm. 97, 152–163. https://doi.org/10.1016/j.ejpb.2015.06.020.
Luo, Q., Zhao, J., Zhang, X., Pan, W., 2011. Nanostructured lipid carrier (NLC) coated with Chitosan Oligosaccharides and its potential use in ocular drug delivery system. Int. J. Pharm. 403, 185–191. https://doi.org/10.1016/j.ijpharm.2010.10.013.
Maupas, C., Moulari, B., Béduneau, A., Lamprecht, A., Pellequer, Y., 2011. Surfactant dependent toxicity of lipid nanocapsules in HaCaT cells. Int. J. Pharm. 411, 136–141. https://doi.org/10.1016/j.ijpharm.2011.03.056.
Messager, S., Goddard, P.A., Dettmar, P.W., Maillard, J.Y., 2001. Determination of the antibacterial efficacy of several antiseptics tested on skin by an “ex-vivo” test. J. Med. Microbiol. 50, 284–292. https://doi.org/10.1099/0022-1317-50-3-284.
Nagoor Meeran, M.F., Jagadeesh, G.S., Selvaraj, P., 2016. Thymol, a dietary monoterpene phenol abrogates mitochondrial dysfunction in β-adrenergic agonist induced myocardial infarcted rats by inhibiting oxidative stress. Chem. Biol. Interact. 244, 159–168. https://doi.org/10.1016/j.cbi.2015.12.006.
Najafloo, R., Behyari, M., Imani, R., Nour, S., 2020. A mini-review of Thymol incorporated materials: Applications in antibacterial wound dressing. J. Drug Deliv. Sci. Technol. 60 https://doi.org/10.1016/j.jddst.2020.101904.
Pham, Q.D., Björklund, S., Engblom, J., Topgaard, D., Sparr, E., 2016. Chemical penetration enhancers in stratum corneum - Relation between molecular effects and barrier function. J. Control. Release 232, 175–187. https://doi.org/10.1016/j.jconrel.2016.04.030.
Pivetta, T.P., Simões, S., Araújo, M.M., Carvalho, T., Arruda, C., Marcato, P.D., 2018. Development of nanoparticles from natural lipids for topical delivery of thymol: Investigation of its anti-inflammatory properties. Colloids Surfaces B Biointerfaces 164, 281–290. https://doi.org/10.1016/j.colsurfb.2018.01.053.
Ramón, E., Alonso, C., Coderch, L., De La Maza, A., López, O., Parra, J.L., Notario, J., 2005. Liposomes as alternative vehicles for sun filter formulations. Drug Deliv. J. Deliv. Target. Ther. Agents 12, 83–88. https://doi.org/10.1080/10717540490446080.
Rincón, M., Calpena, A.C., Clares, B., Espina, M., Garduño-Ramírez, M.L., Rodríguez-Lagunas, M.J., García, M.L., Abrego, G., 2018. Skin-controlled release lipid nanosystems of pranoprofen for the treatment of local inflammation and pain. Nanomedicine 13, 2397–2413. https://doi.org/10.2217/nnm-2018-0195.
Rincón, M., Espinoza, L.C., Silva-Abreu, M., Sosa, L., Pesantez-Narvaez, J., Abrego, G., Calpena, A.C., Mallandrich, M., 2022. Quality by design of pranoprofen loaded nanostructured lipid carriers and their ex vivo evaluation in different mucosae and ocular tissues. Pharmaceuticals 15. https://doi.org/10.3390/ph15101185.
Siboro, S.A.P., Anugrah, D.S.B., Ramesh, K., Park, S.H., Kim, H.R., Lim, K.T., 2021. Tunable porosity of covalently crosslinked alginate-based hydrogels and its significance in drug release behavior. Carbohydr. Polym. 260 https://doi.org/10.1016/j.carbpol.2021.117779.
Silva, C., Ramos-Yacasi, G., Mallandrich, M., Colom-Codina, H., Suñer-Carbó, J., Pérez-González, N., Calpena, A.C., Fernández-Campos, F., 2023. Alginate hydrogel formulation with ketorolac for the treatment of pain related Sialolithiasis. Gels 9. https://doi.org/10.3390/gels9050415.
Souto, E.B., Baldim, I., Oliveira, W.P., Rao, R., Yadav, N., Gama, F.M., Mahant, S., 2020. SLN and NLC for topical, dermal, and transdermal drug delivery. Expert Opin. Drug Deliv. 17, 357–377. https://doi.org/10.1080/17425247.2020.1727883.
Suñer-Carbó, J., Boix-Montañés, A., Halbaut-Bellowa, L., Velázquez-Carralero, N., Zamarbide-Ledesma, J., Bozal-de-Febrer, N., Calpena-Campmany, A.C., 2017. Skin permeation of econazole nitrate formulated in an enhanced hydrophilic multiple emulsion. Mycoses 60, 166–177. https://doi.org/10.1111/myc.12575.
Szwed, M., Torgersen, M.L., Kumari, R.V., Yadava, S.K., Pust, S., Iversen, T.G., Skotland, T., Giri, J., Sandvig, K., 2020. Biological response and cytotoxicity induced by lipid nanocapsules. J. Nanobiotechnol. 18, 1–19. https://doi.org/10.1186/s12951-019-0567-y.
Tayel, K., Attia, M., Agamia, N., Fadl, N., 2020. Acne vulgaris: prevalence, severity, and impact on quality of life and self-esteem among Egyptian adolescents. J. Egypt. Public Health Assoc. 95 https://doi.org/10.1186/s42506-020-00056-9.
Thang, N.H., Chien, T.B., Cuong, D.X., 2023. Polymer-based hydrogels applied in drug delivery: An overview. Gels 9, 523. https://doi.org/10.3390/gels9070523.
Thiboutot, D., Del Rosso, J.Q., 2013. Acne vulgaris and the epidermal barrier: Is acne vulgaris associated with inherent epidermal abnormalities that cause impairment of barrier functions? Do any topical acne therapies alter the structural and/or functional integrity of the epidermal barrier? J. Clin. Aesthet. Dermatol. 6, 18–24.
Thiruchenthooran, V., Świtalska, M., Bonilla, L., Espina, M., García, M.L., Wietrzyk, J., Sánchez-López, E., Gliszczyńska, A., 2022. Novel strategies against cancer: Dexibuprofen-loaded nanostructured lipid carriers. Int. J. Mol. Sci. 23, 11310. https://doi.org/10.3390/ijms231911310.